ИНСТИТУТ ЯДЕРНОЙ ФИЗИКИ СО АН СССР

V.N. Baier, V.M. Katkov and V.M. Strakhovenko

HARD PHOTON EMISSION FROM HIGH ENERGY ELECTRONS AND POSITRONS IN SINGLE CRYSTALS

PREPRINT 91-111

НОВОСИБИРСК

Hard Photon Emission From High Energy Electrons and Positrons in Single Crystals

V.N. Baier, V.M. Katkov and V.M. Strakhovenko

Institute of Nuclear Physics,
630090, Novosibirsk, USSR

A B S T R A C T

A radiation of electrons and positrons in single crystals in coherent bremsstrahlung (CBS) region has been considered for the case when CBS has the most hard spectrum. Under this condition a particle moves near a crystalline plane (in fcc(d) crystal for axis <001> this is the plane $(1\bar{1}0)$) and influence of the continuous plane potential should be taken into account. This potential gives additional contribution in soft part of the spectrum and affects on hard photon emission. Observation of this phenomena at high energy is discussed.

1. INTRODUCTION

The interaction of charged particles and photons with single crystals has been under active theoretical (see e.g. a review [1]) and experimental [2-7] investigation during recent years for energies of projectiles of hundreds GeV. The most detailed experimental analysis was performed for initial particles incident along one of the main crystal axes under channeling conditions or close to that.In this case the radiation process is owing to the action of continuous axis potential being a dozen times more intensive than incoherent radiation which is due to the particle scattering on potential fluctuations (the Bethe-Heitler mechanism). Besides the primary processes of a photon emission by a charged particle and creation of an e^+e^- pair

by a photon the electron-photon showers formation [6] was investigated as well. The characteristic lengths of shower formation turn out to be much shorter in crystals than in corresponding amorphous material owing to significant enhancement of the primary processes in crystals. This property can be used side by side with the specific dependence of the shower characteristics on the angle of incidence ϑ_0 and initial energy to create [8] a small-size detector of ultra-high energy electrons and photons with angular resolution $\Delta\vartheta_0 \leq 10^{-3}$. Note, that the entire set of experimental data obtained is in good agreement with the developed the oretical description [1] of the phenomena mentioned.

Concerning the radiation spectrum in the axis potential, relatively soft photons are mainly radiated even at particle energy ε of hundreds GeV. For example at ε=100 GeV the peak in intensity spectrum is situated for Ge <110> axis at the photon energy (frequency) $\omega \approx 0.05\ \varepsilon$ (see fig. 1 in Ref. [1]). Remind, that the hard peak in electron energy loss distribution observed first in Ref. [3] is owing to high photon multiplicity in a crystal of sufficient thickness, i.e. to the successive emission of a few relatively soft photons registered as one event.

However hard photons can really be emitted by high energy particles in crystals at definite conditions with a probability much higher than in corresponding amorphous

medium. It occurs at the angles of incidence $\vartheta_0 \geq \vartheta_v \equiv V_0/m$ (V_0 is the scale of axis potential, m is the electron mass), when the mechanism of radiation changes. At such angles of incidence one can use the rectilinear trajectory approximation to evaluate characteristics of the particle motion and the qualitative features of the radiation process can be easily analyzed in terms of equivalent photons. Really, in the frame of reference moving with relativistic velocity along the initial particle momentum the crystal field can be represented as a set of the plane electromagnetic waves. As it was emphasized in Ref. [9], the most important distinction between the equivalent photon spectrum in crystal and that in Bethe-Heitler case is the discreteness of the spectrum in crystal and connected to that the existence of a minimal frequency of equivalent photon. The radiation process can be represented as the Compton scattering of equivalent photons on a charged particle. The known theory of coherent bremsstrahlung (CBS) [10, 11] is exhausted by this picture both qualitatively and quantitatively (see e.g. Eq. (4.8) in Ref. [1]). The modification of CBS-theory going beyond the limits of first Born approximation on crystal potential was developed in Ref. [9]. The change of an effective mass of a charged particle moving in the field of a plane electromagnetic wave (a set of such waves in crystal) is additionally taken into account in the modified theory. The 4-momentum conservation

in Compton effect yields:

$$\frac{\omega}{\varepsilon} = \frac{s}{1+s+(\gamma\vartheta_{ph})^2}, \qquad (1.1)$$

here $\gamma=\varepsilon/m$; ϑ_{ph} is the angle between the momentum of outgoing photon and the initial particle momentum $\vec{p}$; $s=2(qp)/m^2$, $(qp)=q_0\varepsilon-\vec{q}\vec{p}$. The momentum q_μ of an initial (equivalent) photon is in the crystal case one of reciprocal lattice vectors $\vec{q}$ taken in a corresponding frame of reference. In the crystal c.m.frame one has: $s = 2\varepsilon|q_\parallel|/m^2$, $q_\parallel = (\vec{q}\vec{p})/|\vec{p}|$. The CBS intensity spectrum has the peak situated just at the boundary (according to Eq. (1.1)) frequency $\omega_b=\varepsilon s/(1+s)$. For different angles of incidence a crystal is characterized by certain set of waves, every one having its own value of the quantity $q_\parallel$. The position of the most soft peak in the CBS intensity spectrum is determined by the minimal value $|q_\parallel|_{min}$ dependent only on the geometric factors. It turns out that at given angle of incidence to the axes ϑ_0 the parameter $|q_\parallel|_{min}$ takes a maximal value, when the particle momentum $\vec{p}$ is in the $(1\bar{1}0)$ plane forming the angle $\vartheta_0 \ll 1$ to the axes <001> for fcc(d)-structure (C, Si, Ge) and to the axes <110> for bcc-structure (W, Fe). Thus, other things being equal, one gets the most hard CBS spectrum when particle is moving under plane channeling conditions or not high above plane potential barrier. In this connection the influence of the field corresponding to the continuous plane potential on the radiation process

should be taken into account. This field in the first place leads to an ordinary radiation at planar channeling giving a contribution to the soft part of the spectrum and secondly affects the emission of hard quanta.

The influence of an external field on Compton effect was considered in Refs. [12-14]. However, the results obtained in [12, 13] can not be applied directly to our case, in particular, because of the initial plane wave was assumed to be unpolarized, when in a crystal equivalent photons are in general polarized. In the next section a straightforward derivation is given of the formulae for radiation spectrum taking into account an action of the external field and the change of the charged particle mass in the plane wave field. The correspondence of this formulae with the results of Ref. [14] is established.

2. DESCRIPTION OF THE RADIATION SPECTRUM UNDER PLANAR CHANNELING CONDITIONS

Let us start from the general formula derived in Ref.[9] for the radiation spectrum at sufficient high energy for arbitrary crystal orientation:

$$\frac{dW_\gamma}{d\omega} = -\frac{i\alpha m^2}{2\pi\varepsilon^2}\int\frac{d^3r_0}{V}F(\vec{r}_0,\vartheta_0)\int_{-\infty}^{\infty}\frac{d\tau}{\tau-i0}\Bigg[\Bigg(\sum_{\vec{q}}\frac{G(\vec{q})\vec{q}_\perp}{mq_\parallel}\sin(q_\parallel\tau)\times$$

$$\times e^{-iq\vec{r}(t)}\Big)^{2\beta-1}\Big]e^{-iA}, \qquad (2.1)$$

here $\beta=\varepsilon/\varepsilon'+\varepsilon'/\varepsilon$, $\varepsilon'=\varepsilon-\omega$; $q_{\parallel}=(\vec{q}\vec{v}_0)$, $\vec{v}_0$ is the mean velocity of the particle traversing a crystal; $\vec{r}(t)=\vec{r}+t\vec{v}_0$; $\alpha=1/137$ is the fine structure constant; the crystal potential is used in the form of $U(\vec{r})=\sum G(\vec{q})e^{-iq\,r}$;

$$A=\frac{m^2\omega\tau}{\varepsilon\varepsilon'}\Bigg\{1+\sum_{\vec{q},\vec{q}'}\frac{G(\vec{q})G(\vec{q}')}{m^2 q_{\parallel} q'_{\parallel}}(\vec{q}_{\perp}\vec{q}'_{\perp})\Bigg[\frac{\sin(q_{\parallel}+q'_{\parallel})\tau}{(q_{\parallel}+q'_{\parallel})\tau}-$$

$$-\frac{\sin(q_{\parallel}\tau)}{q_{\parallel}\tau}\cdot\frac{\sin(q'_{\parallel}\tau)}{q'_{\parallel}\tau}\Bigg]e^{-i(\vec{q}+\vec{q}',\vec{r}(t))}\Bigg\}. \qquad (2.2)$$

The function $F(\vec{r},\ \vartheta_0)$ in Eq. (2.1) gives the coordinate distribution depending on the parameters of the incident beam and generally speaking on time. Below the crystal is assumed to be thin i.e. the kinetics of this distribution is neglected. As it was shown in [14] the problem of a photon emission by a charged particle in simultaneously acting a plane wave field and an external one can be solved analytically only if the radiation in a pure external field has the magnetic bremsstrahlung nature. For that in the case under consideration the parameter $\rho_c=2U_0\varepsilon/m^2$ where U_0 is the potential well depth should be large: $\rho_c\gg 1$, and the angle Ψ

of the particle velocity $\vec{v}_0$ to the plane should satisfy the condition $\Psi\le U_0/m$. When the angle ϑ_0 of the vector $\vec{v}_0$ to the chosen axis is small, the contribution to the sum $\sum_{\vec{q}}$ is given by the vectors $\vec{q}_t$ situated in the plane perpendicular to this axis, i.e. all the sums become two-dimensional. The continuous planar potential corresponds to the terms in the sum with $\vec{q}_t$ perpendicular to the plane. To separate this contribution we split all the sums into two parts: $\sum_{\vec{q}}\longrightarrow\sum_{\vec{q}_t}\equiv\sum_{\vec{q}_t}^{(F)}+\sum_{\vec{q}_t}^{(w)}$, where the sum $\sum_{\vec{q}_t}^{(F)}$ contains $\vec{q}_t$ for which $q_{\parallel}\longrightarrow 0$ when $\Psi\longrightarrow 0$, and the sum $\Sigma^{(w)}$ contains all the others $\vec{q}_t$. The functions contained in the sum $\Sigma^{(F)}$ can be expanded in powers of $|q_{\parallel}|\tau\ll 1$. After that this sum is expressed in terms of continuous planar potential $U(y)=\sum_{\vec{q}_y}G(\vec{q}_y)\,e^{-iq_y y}$, where y is the coordinate perpendicular to the plane. Carrying out these transformations and changing $\tau\longrightarrow\tau\varepsilon/m^2$ we get from Eq. (2.1):

$$\frac{dW_\gamma}{dx}=\frac{i\alpha m^2}{2\pi\varepsilon}\int\frac{d^2\rho_0}{S_0}F(\vec{\rho}_0,\vartheta_0)\int_{-\infty}^{\infty}\frac{d\tau}{\tau-i0}\Big[1+\beta\tau^2(\vec{\chi}+\vec{C})^2\Big]\times$$

$$\times\exp\Big\{-i u\tau\Big[1+\tau^2\vec{\chi}^2/3-4(\vec{\chi}\vec{A})-(\vec{B})^2+\rho/2+\tilde{\Sigma}\Big]\Big\}, \qquad (2.3)$$

here $\vec{\rho}_0$ is the coordinate vector in the plane perpendicular to the chosen axis, S_0 is the area per one axis, over which coordinate averaging is carried out, the quantity β is de-

termined in Eq. (2.1), $u=\omega/\varepsilon'$, $x=\omega/\varepsilon$,

$$\begin{Bmatrix}\vec{A}\\ \vec{B}\\ \vec{C}\end{Bmatrix} = \sum_{\vec{q}_t}^{(w)} G(\vec{q}_t)\,\vec{q}_t \frac{}{mq_\parallel} e^{-i\,\vec{q}_t\vec{r}(t)} \begin{Bmatrix} if_2(s)/s \\ f_1(s) \\ isf_1(s)/2 \end{Bmatrix},$$

$s=2q_\parallel\varepsilon/m^2$, $s'=s(q'_\parallel)$

$f_1(s)=2\sin(s\tau/2)/s\tau$, $f_2(s)=\cos(s\tau/2)-f_1(s)$, (2.4)

$$\vec{\chi}=\frac{i\varepsilon}{m^3}\sum_{\vec{q}_y} G(\vec{q}_y)\,\vec{q}_y e^{-iq_y y},\quad \rho/2=\sum_{\vec{q}_t,\, q_\parallel\neq 0}^{(w)} |G(\vec{q}_t)/m|^2 (\vec{q}_t/q_\parallel)^2$$

$$\tilde{\Sigma} = \sum_{\vec{q}_t,\vec{q}_t}^{(w)} \frac{G(\vec{q}_t)G(\vec{q}'_t)}{m^2 q_\parallel q'_\parallel} (\vec{q}_t\vec{q}'_t)\Big[f_1(s+s')-$$

$$-\delta_{\vec{q}_t+\vec{q}'_t,0}\Big] e^{-i(\vec{r}(t),\vec{q}_t+\vec{q}'_t)}.$$

Note, that $|\vec{\chi}| = \varepsilon m^{-3}|dU/dy| = \varepsilon m^{-3}|eE(y)| = \varepsilon|E(y)|/(mE_0)$, where $E(y)$ is a magnitude of the electric field of the plane at the distance y from it, $E_0=m^2/e \cong 1.32\cdot 10^{16}$ V/cm is the critical field. This coincides with the standard definition of the quantum parameter χ characterizing the properties of magnetic bremsstrahlung. If we denote time averaging by $\langle\ldots\rangle$, then the parameter $\rho/2$ characterizing in particular the intensity of an electromagnetic wave can be written in

the form of

$$\rho/2=\Big\langle \sum_{\vec{q}_t,\vec{q}'_t}^{(w)} \frac{G(\vec{q}_t)G(\vec{q}'_t)}{m^2 q_\parallel q'_\parallel} (\vec{q}_t\vec{q}'_t) f_1(s+s') e^{-i(\vec{r}(t),\vec{q}_t+\vec{q}'_t)}\Big\rangle,$$

i.e. the average value of the first term in the double sum $\Sigma^{(w)}$ in Eq. (2.2) has been isolated in Eq. (2.3). Note more, that the average value of the quantity $\tilde{\Sigma}$ is equal to zero. The Eq. (2.3) completely corresponds to Eq. (8) of Ref. [14], if we substitute in the latter a set of crystal waves in place of one wave and let $\vec{\zeta}=0$, since in Eq. (2.3) an initial particle is assumed to be unpolarized. The exponential function in Eq. (2.3) can be expanded in the wave fields (terms containing $\Sigma^{(w)}$). At $\vartheta_0 \gg \vartheta_v$ such expansion is valid (see discussion in section 4 of Ref. [1]) at arbitrary photon frequency. When $|s|\gg 1$ it is valid in a neighborhood of the hard peak position for $\vartheta_0 \geq \vartheta_v$ as well. Carrying out this expansion, we find after time averaging:

$$\frac{dW}{dx}\gamma = \frac{i\alpha m^2}{2\pi\varepsilon}\int \frac{dy}{d_{p1}} F(y,\vartheta_0) \int_{-\infty}^{\infty} \frac{d\tau}{\tau-i0} \times$$

$$\times\exp\Big[-iu\tau\Big(1+\rho/2+\tau^2\chi^2/3\Big)\Big]\cdot\Big\{1+\beta\tau^2\chi^2+$$

$$+\sum_{\vec{q}_t}^{(w)}\frac{\left|G(\vec{q}_t)\right|^2}{m^2q_{\parallel}^2}\vec{q}_t^{\,2}\left[\left(1+\beta\tau^2\chi^2\right)\cdot\left(iu\tau f_1^2(s)-4\Lambda_1(f_2(s)u\tau\mu)^2\right)+\right.$$

$$\left.+\beta\cdot\left(\sin(s\tau/2)+4iu\Lambda_1\tau^2\mu^2sf_2(s)\right)\cdot\sin(s\tau/2)\right], \qquad (2.5)$$

here d_{pl} is the distance between the planes, near which the motion occurs; $\Lambda_1=2(\vec{\chi}\vec{q}_t)^2/\chi^2\vec{q}_t^{\,2}$, $\mu=\chi/|s|$. In what follows we assume the parameter s to be positive: $s\to|s|=2\varepsilon|q_{\parallel}|/m^2$, since the integrand in Eq. (2.5) is an even function of s. In the case of one wave considered in Ref. [14], the parameter Λ_1 has the following form: $\Lambda_1=1+\lambda_3\cos(2\phi_1)$, where ϕ_1 is the angle of the wave polarization vector to the external field direction, and λ_3 is the degree of wave linear polarization. A comparison of this expression for Λ_1 with one obtained in a crystal case proves, that equivalent photons in a crystal are completely polarized ($\lambda_3=1$) along the direction $\vec{q}_t$. The parameter μ characterizes (see Ref. [14]) the strength of an external field in the sense of it's influence on the Compton scattering of wave photons (on the coherent radiation in a crystal). The order of magnitude of the parameter μ is the ratio of the momentum transferred by an external field to a charged particle on the wave length to it's mass.

By integrating in Eq. (2.5) over τ it is convenient to go over to the variable $z=|s|\tau$ and to carry out the

integration by parts of terms containing high powers of τ. All the integrals are taken by means of the formula:

$$\frac{1}{2\pi i}\int_{-\infty}^{\infty}\frac{dz}{z-i0}e^{-i(zt+\lambda^2z^3/3)}=\frac{\vartheta(t)}{\pi\sqrt{3}}\int_a^{\infty}dx\,K_{\frac{1}{3}}(x)+\vartheta(-t)\left[1-\right.$$

$$\left.-\frac{1}{3}\int_a^{\infty}dx\left(J_{\frac{1}{3}}(x)+J_{-\frac{1}{3}}(x)\right)\right] \qquad (2.6)$$

and relations obtained from it by differentiating with respect to t. In Eq.(2.6) J_ν are the Bessel functions of the first kind, and K_ν are the Bessel functions of the third kind (MacDonald functions); $a=2t^{3/2}/3\lambda$. The integration over τ in Eq. (2.5) yields:

$$\frac{dW_\gamma}{dx}=\frac{\alpha m^2}{\pi\varepsilon\sqrt{3}}\int\frac{dy}{d_{pl}}F(y,\vartheta_0)\left\{(1+\rho/2)\cdot\beta\cdot K_{\frac{2}{3}}(z_0)-\int_{z_0}^{\infty}dx\,K_{\frac{1}{3}}(x)+\right.$$

$$\sum_{\vec{q}_t}^{(w)}\frac{\left|G(\vec{q}_t)\right|^2}{m^2q_{\parallel}^2}\vec{q}_t^{\,2}\left\{(g_1+\nu)\int_{z_+}^{\infty}dx\,K_{\frac{1}{3}}(x)-2g_1\int_{z_0}^{\infty}dx\,K_{\frac{1}{3}}(x)+\right.$$

$$(g_1-\nu)\left[\vartheta(u-u_0)\int_{z_-}^{\infty}dx\,K_{\frac{1}{3}}(x)+\pi\sqrt{3}\,\vartheta(u_0-u)\left(1-\frac{1}{3}\int_{z_-}^{\infty}dx(J_{\frac{1}{3}}(x)+\right.\right.$$

$$+J_{-\frac{1}{3}}(x))\Big)\Big]+\mu\nu(3\chi/2u)^{1/3}\Big[(g_4+4\nu g_2)z_+^{1/3}\,K_{\frac{1}{3}}(z_+)-2\beta(1-\Lambda_1)z_0^{1/3}\cdot$$

$$K_{\frac{1}{3}}(z_0)+(g_4-4\nu g_2)\Big(\vartheta(u-u_0)K_{\frac{1}{3}}(z_-)+\frac{\pi}{\sqrt{3}}\vartheta(u_0-u)(J_{\frac{1}{3}}(z_-)+J_{-\frac{1}{3}}(z_-))\Big)\cdot$$

$$z_-^{1/3}\Big]+\nu^2(3\chi/2u)^{2/3}\Big[(g_2-g_3)z_+^{2/3}\,K_{\frac{2}{3}}(z_+)+2(g_2+g_3)z_0^{2/3}\,K_{\frac{2}{3}}(z_0)+$$

$$+(g_2-g_3)z_-^{2/3}\Big(\vartheta(u-u_0)K_{\frac{2}{3}}(z_-)+\frac{\pi}{\sqrt{3}}\vartheta(u_0-u)(J_{-\frac{2}{3}}(z_-)-J_{\frac{2}{3}}(z_-))\Big)\Big]\Big\}\Big\}\,, \qquad (2.7)$$

here $\vartheta(z)$ is the Heviside function: $\vartheta(z)=1$ for $z>0$ and $\vartheta(z)=0$ for $z<0$, the notations are introduced:

$$z_0=(2u/3\chi)(1+\rho/2)^{3/2},\quad z_\pm=z_0(1\pm u_0/u)^{3/2},\quad u_0=|s|/(1+\rho/2),$$

$$g_1=\beta/4+\nu^2(1+\rho/2-4\Lambda_1\mu^2)\,,\quad g_2=\Lambda_1[\,\beta(1+\rho/2)-1]\,, \qquad (2.8)$$

$$g_3=1-4\Lambda_1\beta\mu^2,\quad g_4=\beta(1+\Lambda_1)\,,\quad \nu=u/|s|\,.$$

The terms in Eq. (2.7) outside of the sum $\Sigma^{(w)}$ represent usual magnetic bremsstrahlung in the field of a plane slightly corrected owing to the presence of waves. In the argument z_0 this correction is reduced to the substitution: $m^2\longrightarrow m_{ef}^2=m^2(1+\rho/2)$ since the parameter $\chi\sim m^{-3}$. The same

correction happens in the parameter u_0, determining a boundary of the Compton spectrum at given frequency of an initial photon (at given value of the quantity $q_\parallel$ in our case). A transition from Eq.(2.7) to the case of one wave is provided by the substitution: $\Sigma^{(w)}|G(\vec{q}_t)\,\vec{q}_t|^2/m^2q_\parallel^2\longrightarrow\rho/2=\xi_0^2$, where ξ_0^2 is the intensity of this wave, and if the change of the mass m to the effective value m_{ef} is not taken into account, by the additional expansion of the terms describing the magnetic bremsstrahlung in $\rho/2$. An expression obtained in this way is consistent with the results of Ref. [14]. In the case of a strong external field ($\mu=\chi/s\gg1$) the Eqs. (2.3) and (2.7) are reduced (see Ref. [14]) to the formulae of the magnetic bremsstrahlung, where one should add together vectors of accelerations induced by an external field and a wave field, to determine the parameter χ.

In the case of a weak field ($\mu\ll1$), which is practically more interesting, it influences most strongly on the coherent radiation spectrum near the intensity peak of the latter, i.e. at $u\cong u_0$. The Eq. (2.7) implies at $\mu\ll1$ the spectrum variation of the order of unity for photon frequencies satisfying the condition $|u-u_0|\le\mu^{2/3}$. This is physically explained by the fact, that the length of coherent radiation formation $l_w\sim|u-u_0|^{-1}$ (see [14]). Then the length l_w becomes larger than the corresponding formation length in an external field $l_f\sim\chi^{-1}(1+\chi/u)^{1/3}$ at sufficiently small distances from the boundary frequency. This means the

change of the radiation mechanism within the mentioned range of frequencies. The considered change of the intensity spectrum is illustrated by Fig. 1 in one wave and weak external field case. Then the probability (first Born approximation in wave) can be represented as:

$$\frac{dW_\gamma}{dx} = \frac{dW_\gamma^{(F)}}{dx} + \xi_0^2 \frac{dW_\gamma^{(w)}}{dx} , \qquad (2.9)$$

where the first term describes the magnetic bremsstrahlung induced by an external field. Note, that Eq. (2.7) has the same form, but in contrast to Eq. (2.9) a set of waves is substituted, and as it was explained above, the term $dW_\gamma^{(w)}/dx$ is slightly changed. The part of the probability proportional to ξ_0^2 in Eq. (2.9) can be interpreted by usual rules in terms of a cross-section:

$$d\sigma = \frac{8\pi\alpha\varepsilon}{m^4 s} dW_\gamma^{(w)} , \qquad (2.10)$$

i.e. we can discuss a change of the Compton scattering in an external field. Eq. (2.7) implies, that this cross-section at μ tending to zero is reduced to the ordinary Compton formula multiplied by the factor

$$f(u)=\frac{\vartheta(u-u_0)}{\pi\sqrt{3}}\int_z^\infty dx\ K_{\frac{1}{3}}(x) + \vartheta(u_0-u)\left[1-\frac{1}{3}\int_z^\infty dx\ \left(J_{\frac{1}{3}}(x) + J_{-\frac{1}{3}}(x)\right)\right],$$

which noticeably differs from unity in the narrowing (at $\mu \longrightarrow 0$) neighborhood of the point $u=u_0$, where $f(u_0)=1/3$. The function $I^{(w)} = \xi_0^2 \cdot x\ dW_\gamma^{(w)}/dx$ is shown in Fig. 1 for two values of the parameter $\mu=\chi/s$. It was calculated taking into account all the terms in the probability $dW_\gamma^{(w)}$. It is seen, that oscillations arise in the mono-tone (at $\chi=0$) spectral curve, the peak is lowering and moving to the left from the point $u=s$, and the tail of the distribution appears in the kinematically prohibited (at $\chi = 0$) frequency domain $u > s$. The scale of these alterations increases with increase of the parameter μ.

3. DISCUSSION AND CONCLUSIONS

According to what has been said in Introduction we consider the radiation process for initial particle velocity $\vec{v}_0$ being nearly aligned with the axis <001> for the crystal structure fcc (d). Let ϑ_0 be the angle of the vector $\vec{v}_0$ to this axis, and ϕ_0 be the angle of the projection $\vec{v}_0$ onto the plane (001) to the plane $(1\bar{1}0)$. Remind, that l is the lattice constant and $\vec{q}=2\pi/l\cdot(m, n, k)$, where m, n and k are integers. For the axis <001> the quantities $\vec{q}_t$ and $q_\parallel$ have the form:

$$\vec{q}_t = \frac{2\pi}{l}(m,n,0) , \quad q_\parallel = \frac{\pi\sqrt{2}}{l} \sin\vartheta_0[(m+n)\cos\phi_0+(m-n)\sin\phi_0] .$$

Similarly, in the case of the crystal structure (bcc) we

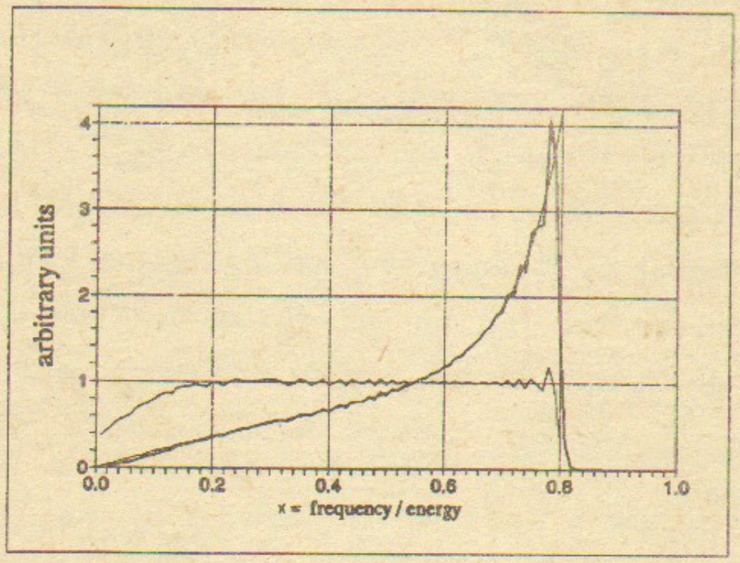

Fig. 1. Intensity spectra $x \cdot dW_{\gamma}^{(W)}/dx$ for $s = 4$ in the absence (χ=0) of an external field (dotted), in the presence of the field (heavy solid), and their ratio (solid) at $\chi = 0.04$ in Fig. 1*a* and at $\chi = 0.3$ in Fig. 1*b*.

consider the radiation from particles nearly aligned with the <110> axis. Then ϑ_0 is the angle of velocity $\vec{v}_0$ to this axis, and ϕ_0 is the angle of the projection $\vec{v}_0$ onto the plane $(1\bar{1}0)$ to the plane (110), and

$$\vec{q}_t = \frac{2\pi}{l}(m,-m,k)\ , \quad q_{\parallel} = \frac{2\pi}{l}\sin\vartheta_0[k\cdot\cos\phi_0 + m\sqrt{2}\ \sin\phi_0]\ .$$

Let us start with the ordinary situation, when the influence of the plane field on the radiation process can be neglected. In general, for $\vartheta_0 \ll 1$ there is always a plane containing the chosen axis and having the angle ψ to the velocity $\vec{v}_0$ less than the corresponding critical angle of planar channeling ψ_c. However, it is possible to avoid the main planes. For example, at $\sin\phi_0$=0.25 (see Fig. 2) the angle ψ to the plane $(\bar{3}50)$ for ϑ_0=0.3 mrad is only 2.34 μrad being less than corresponding ψ_c value. But as far as this plane is very weak ($U_0 \simeq$ 1.2 eV, $\chi_{max} \simeq$ 0.037), it's field influence on coherent radiation is small, roughly like that shown in Fig. 1a. Therefore the calculation of curves presented in Fig. 2 was carried out for μ=0 (χ=0), when Eq. (2.7) coincides with the expression (see Eq. (4.1) in Ref. [1]) obtained within modified coherent bremsstrahlung theory. It is seen in Fig. 2, that the peaks become harder, and their heights diminish, when the angle ϑ_0 is increased. The peaks shift to the right due to the proportional in ϑ_0 increase of the parameter s (see Eq. (1.1)). The diminution

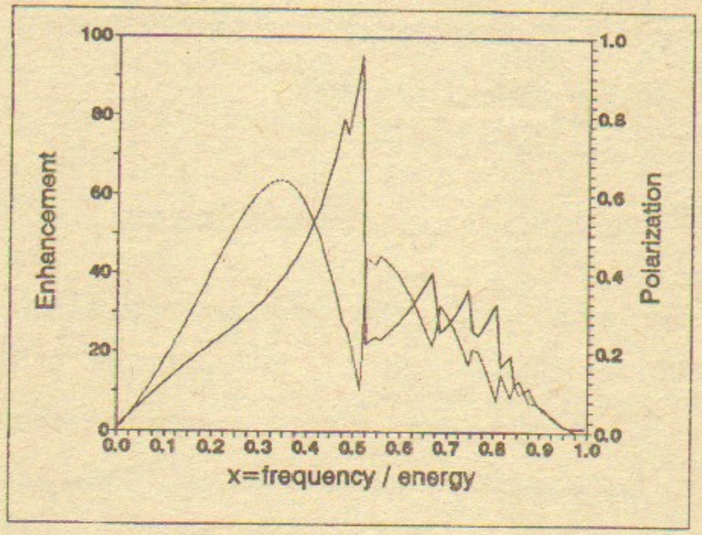

a

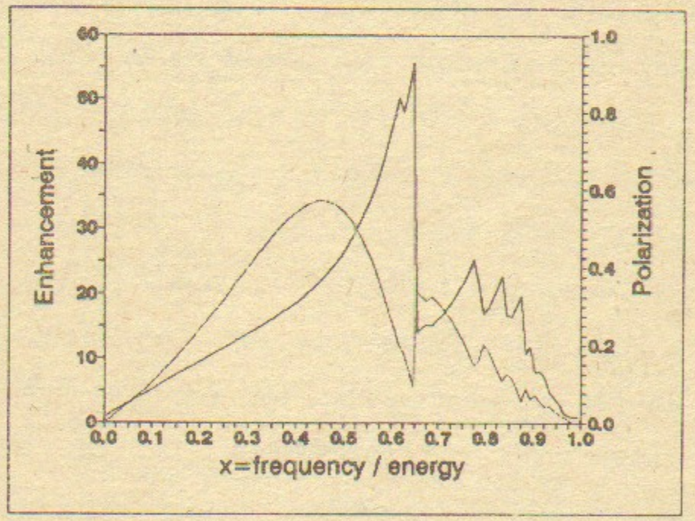

b

Fig. 2. Enhancement (solid) and linear polarization degree (dashed) of the radiation from particles moving close to the <001> axis of a diamond crystal at $\varepsilon = 200$ GeV, $\sin \phi_0 = 0.25$; for $\theta_0 = 0.3$ mrad in Fig. 2*a* and for $\theta_0 = 0.5$ mrad in Fig. 2*b*.

of their heights is owing to the increasing strength of interaction (increasing value of the parameter $\rho/2$). The arising radiation has an essential linear polarization. The spectral distribution of the polarization degree is also shown in Fig. 2. Note, that the maxima of an enhancements (peaks) are situated at the same frequencies as the minima of the polarization degree. The enhancement means the ratio of the spectrum calculated for crystal to the theoretical value of the spectrum in the corresponding amorphous material.

The similar change of the shape in the hard part of the spectrum occurs at increasing angle ϑ_0, when particles are moving close to the strong $(1\bar{1}0)$-plane. It can be seen in Fig. 3. The calculation of curves presented in this figure was carried out by Eq. (2.7) for uniform distribution, i.e. letting $F(y, \vec{v}_0)=1$. The particles moving over a potential barrier approximately have the distribution like that. The angle ψ of the vector $\vec{v}_0$ to the plane $(1\bar{1}0)$ is expressed by means of the angles ϑ_0 and ϕ_0: $\psi \simeq \vartheta_0 \sin \phi_0$. The calculation shows, that the shape of the spectrum is practically not changed by the variation of the angle ϕ_0, which remain valid the inequality $\psi_c < \psi < U_0/m$. On the other hand for $\psi < \psi_c$ one should take into account the particle flux redistribution $(F(y, \vec{v}_0) \neq 1)$, while for $\psi > U_0/m$ the radiation induced by the plane field necessarily looses it's magnetic bremsstrahlung nature, and the developed description of the field influence

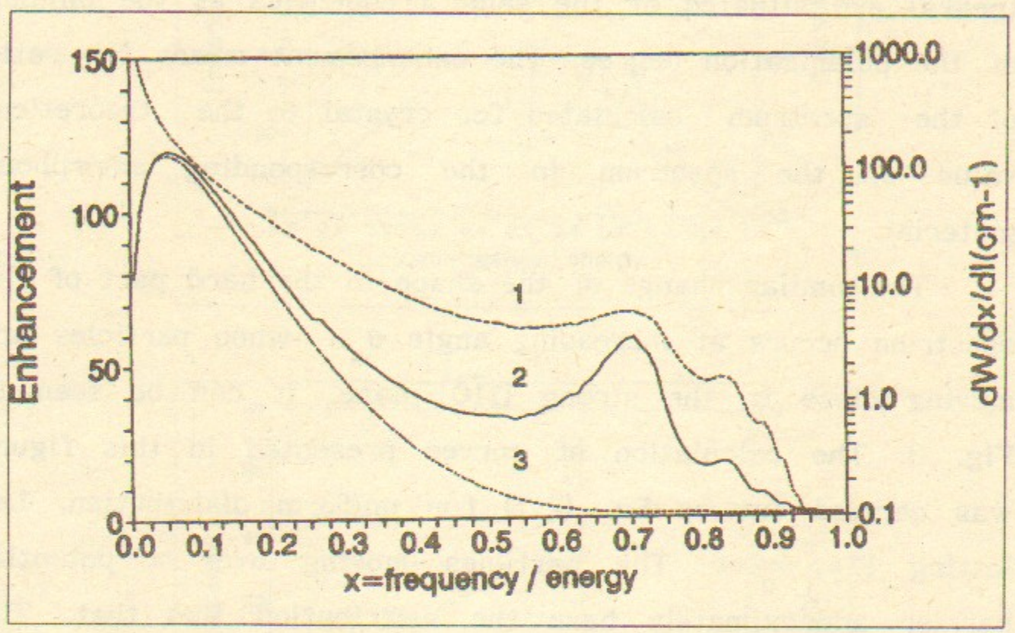

a

Fig. 3. Probability (dashed (1)), enhancement (solid (2)) and (in Fig. 3*a* only) constant field contribution (dotted (3)) for the radiation from particles moving close to the <001> axis and (1$\bar{1}$0) plane of a diamond crystal at $\varepsilon = 200$ GeV, $\psi \geq 15$ mrad; for $\theta_0 = 0.2$ mrad in Fig. 3*a*, $\theta_0 = 0.4$ mrad in Fig. 3*b* and $\theta_0 = 0.6$ mrad in Fig. 3*c*.

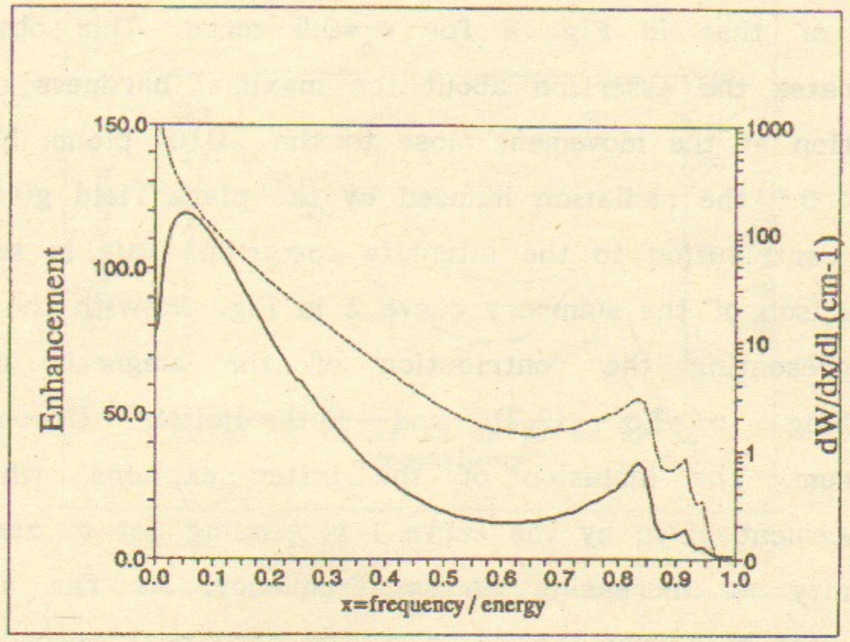

b

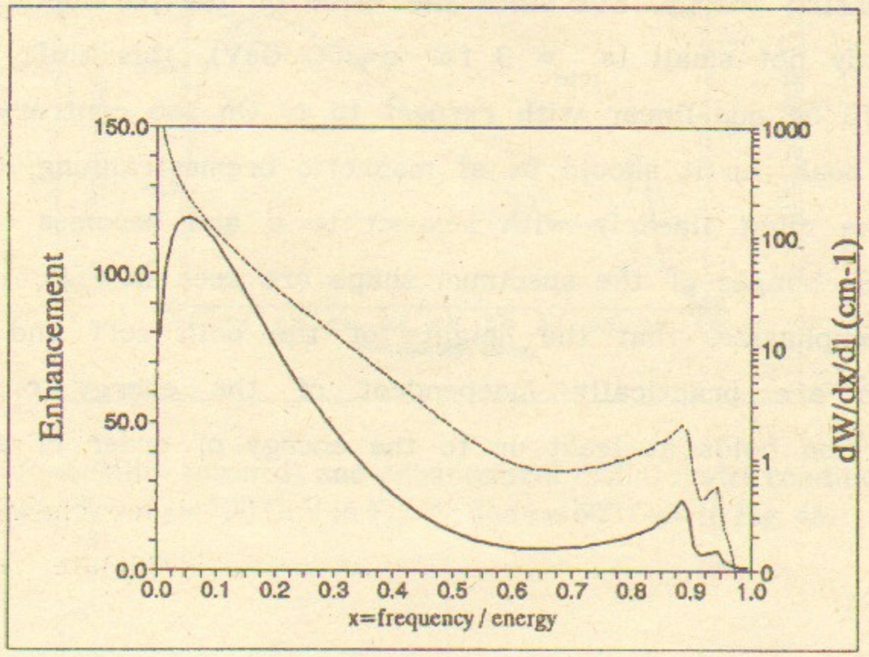

c

on coherent bremsstrahlung becomes inapplicable. The hard peak in Fig. 3even though for ϑ_0=0.2 mrad is situated to the right of that in Fig. 2 for ϑ_0=0.5 mrad. This obviously illustrates the assertion about the maximal hardness of the radiation at the movement close to the $(1\bar{1}0)$ plane. For x= ω/ε < 0.5 the radiation induced by the plane field gives the main contribution to the intensity spectrum. This is seen at comparison of the summary curve 2 in Fig. 3a with the curve 1 representing the contribution of the magnetic brems-strahlung in Eq. (2.7) and Bethe-Heitler (incoherent) spectrum. The inclusion of the latter explains, why the enhancement given by the curve 1 is tending not to zero but to unity at increasing photon frequency. As far as the parameter s is proportional to ε, the hard peak according to Eq. (1.1) moves to the right proportionally to s/(1+s) at increasing energy. But since the value of the parameter s is already not small ($s_{min} \simeq 3$ for ε=200 GeV), this shift turns out to be non-linear with respect to ε. On the contrary, the soft peak, as it should be at magnetic bremsstrahlung, moves to the right linearly with respect to ε and becomes wider. These changes of the spectrum shape are seen in Figs. 3a, 4. We emphasize, that the heights of the both soft and hard peaks are practically independent of the energy ε. This assertion holds at least up to the energy of order of a few TeV.

a

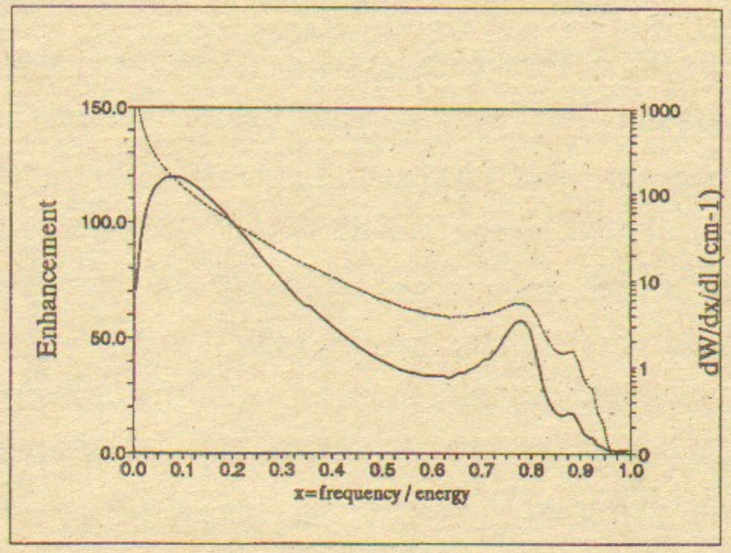

b

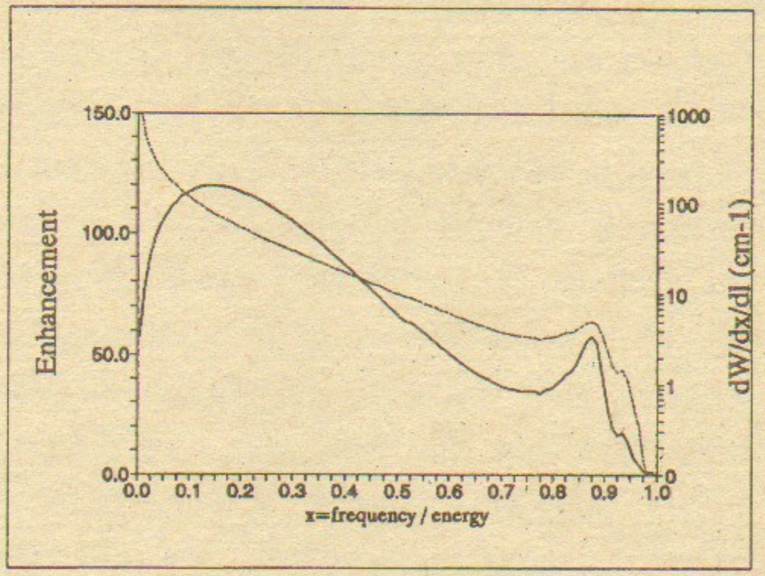

Fig. 4. Probability (dashed) and enhancement (solid) under conditions of Fig. 3*a*; at ε = 300 GeV in Fig. 4*a* and ε = 600 GeV in Fig. 4*b*.

It is well known, that the radiation from channeled electrons and positrons turns out to be different, since they move in different potentials. Channeled electrons are focused around the planes (flux redistribution) moving on the average in the stronger field. On the contrary the coherent radiation from electrons and positrons is usually the same. In the case under consideration the field of the plane causes a difference in the radiation from e^+ and e^- in the hard part of the spectrum as well. The spectra from e^+ and e^- are shown in Fig. 5 for Ge and W crystals at $\phi_0=0$ ($\psi=0$). The difference of two spectra (from e^+ and e^-) is about (10-15)% in the vicinity of the hard peak position being maximal for W crystal. The magnetic bremsstrahlung contribution is negligibly small in this frequency region, therefore the mentioned difference is completely stipulated by the influence of the field on the coherent radiation process, which is actually Compton scattering of equivalent photons on particles of the incident beam. The experimental observation of this difference could verify the possibility of the external field **influence** on one of the fundamental QED-process, what has not been seen up to now. High crystal quality is necessary for an experiment of such kind, in particular the mosaic spread and the accuracy of the angle ψ measurement should be a few times less than the critical angle ψ_c. The requirements are not so rigid for an observation of the spectra like these in Figs. 3 and 4, but

a

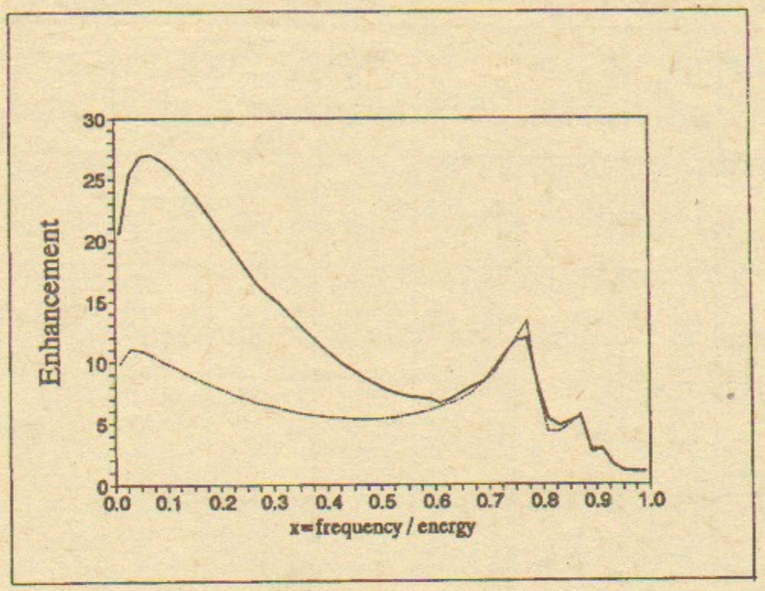

b

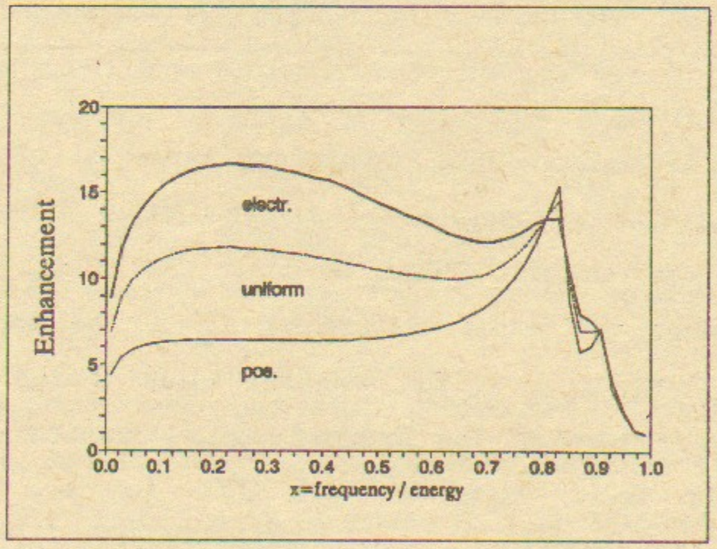

Fig. 5. *a)* – Enhancement for electrons (solid) and positrons (dashed) channeled in Ge $(1\bar{1}0)$ plane close to <001> axis at $\varepsilon = 200$ GeV, $\theta_0 = 0.4$ mrad; *b)* – enhancement for electrons and positrons channeled in W $(1\bar{1}0)$ plane close to <110> axis at $\varepsilon = 200$ GeV, $\theta_0 = 0.5$ mrad, the dashed curve is calculated for uniform distribution.

Table

Crystal type	ψ_c μrad	U_0/m μrad	χ_{max}	ϑ_0 mrad	L_{ch}^{-1} cm^{-1}	x_{max}	r	w cm^{-1}
C fcc(d)	15.3	46	0.24	0.2	4.3	0.71	58.4	6.1
Si fcc(d)	14.6	42	0.17	0.3	2.1	0.72	22.0	2.9
Ge fcc(d)	18.2	65	0.28	0.4	4.4	0.76	11.8	6.1
Fe bcc	26.2	135	0.55	0.35	11.8	0.77	20.3	13.5
W bcc	36.5	250	1.28	0.5	29.9	0.81	14.4	46.2

Parameters characterizing continuous potential of the $(1\bar{1}0)$ plane and some properties of the radiation from particles moving close to this plane at ε = 200 GeV; ψ_c is the critical angle of planar channeling, U_0 is the depth of the potential well, χ_{max} is the maximal value of the parameter χ, ϑ_0 is the angle of the incident particle momentum to axes (<001> for fcc(d) structure and <110> for bcc structure), L_{ch} is the radiation length under indicated conditions, $x_{max} = \omega_{max}/\varepsilon$ is the hard peak position, r is the magnitude of the enhancement at $x=x_{max}$, w is the magnitude of the probability $d^2W/dx\,dl$ at $x=x_{max}$.

in every case the mosaic spread should not exceed the value U_0/m. The values of the angles ψ_c and U_0/m are listed in the Table for the $(1\bar{1}0)$ plane of some crystals. Some characteristics of radiation calculated for uniform distribution $(F(y, \vec{v}_0)=1)$ are also given in the Table.

An increase of the nucleus charge Z leads for identical crystal structure to decreasing enhancement for all the frequencies, so that the maximal enhancement is achieved in diamond. The magnitude of the radiation probability in the vicinity of the peak may serve as more objective characteristic of a crystal fitness for hard photons production. It is seen in the Table, that this probability has not monotone behavior with respect to Z being maximal for tungsten. The maximal values of the parameter χ depending on a distance from the plane are also given in the Table. It is clear, that the effective χ value at averaging over this distance is less than χ_{max}. Note, that the field of the plane accounts for about 2/3 of the quantity L_{ch}^{-1} characterizing the rate of particle energy loss for all examples in the Table.

Thus, the most preferable situation for hard photons production is realized, when incident particles move close to the $(1\bar{1}0)$ plane of a crystal. If the soft part of the spectrum arising under these conditions is undesirable, the crystal orientation can be chosen like that used by obtaining Fig. 2, i.e. one should avoid the main planes.

The experimental investigation of the phenomena discussed above is highly desirable. It could allow one to conclude on the possibility of hard photon sources based on the considered effects, and to verify our understanding of QED processes in strong external fields.

REFERENCES

1. *V.N. Baier, V.M. Katkov and V.M. Strakhovenko.* Sov. Phys. Usp. 32 (1989) 972.
2. *A. Belkacem et al.* Phys. Rev. Lett. 54 (1985) 2667.
3. *A. Belkacem et al.* Phys. Lett. B 177 (1986) 211.
4. *A. Belkacem et al.* Phys. Rev. Lett. 58 (1987) 1196.
5. *J.F. Bak et al.* Phys. Lett. B 202 (1988) 615.
6. *R. Medenwaldt et al.* Phys. Lett. B 227 (1989) 483.
7. *R. Medenwaldt et. al.* Phys. Rev. Lett. 63 (1989) 2827.
8. *V.N. Baier, V.M. Katkov and V.M. Strakhovenko.* Nucl. Instrum. Methods A 250 (1986) 514.
9. *V.N. Baier, V.M. Katkov and V.M. Strakhovenko.* Sov. Phys. JETP 65 (1987) 686.
10. *M.L. Ter-Mikaelyan.* Influence of the medium on electromagnetic processes at high energies (in Russian), Publishing house of the armenian academy of sciences, Erevan, 1969.
11. *G. Diambrini-Palazzi.* Rev. Mod. Phys. 40 (1968) 611.
12. *V.Ch. Zhukovsky and I. Hermann.* Yad. Fiz. 14 (1971) 150.
13. *V.Ch. Zhukovsky and N.S. Nikitina.* Zh. Eksp. Teor. Fiz. 64 (1973) 1169.
14. *V.N. Baier, V.M. Katkov and V.M. Strakhovenko.* Quasiclassical theory of electromagnetic processes in a plane wave field and a constant field, Preprint INP 91-32, Novosibirsk, 1991. Zh. Eksp. Teor. Phys. 100 (1991) 1713.

V.N Baier, V.M. Katkov, V.M. Strakhovenko

**Hard Photon Emission from
High Energy Electrons and Positrons
in Single Crystals**

В.Н. Байер, В.М. Катков, В.М. Страховенко

**Излучение жестких фотонов
электронами и позитронами высокой энергии
в монокристаллах**

Ответственный за выпуск С.Г. Попов

Работа поступила 23 октября 1991 г.
Подписано в печать 25.10. 1991 г.
Формат бумаги 60×90 1/16 Объем 2,2 печ.л., 1,8 уч.-изд.л.
Тираж 250 экз. Бесплатно. Заказ N 111

Ротапринт ИЯФ СО АН СССР,
Новосибирск, 630090, пр. академика Лаврентьева, 11.